Hillside geophysics report

Lancaster Environment Centre | Lancaster University

Survey Personnel

Field Coordinator:	Andrew Binley
Report Author:	Andrew Binley
Field Assistants:	Vassil Karloukovski (Lancaster University)

Dates

Fieldwork:	22 February, 8 & 18 March 2022
Report:	16 August 2023

NGR	SD 47272 61931
W3W	sling.shell.gender
Location	The site is located at the front of 4,5 & 6 Hillside, Lancaster, LA1 1YH.
Survey Methods	Ground penetrating radar (GPR).
Study Area	0.05 ha.

Aims

To identify any geophysical anomalies that may provide evidence of elements of former Roman fortification defences along the western edge of the Lancaster Roman fort and identify any features from one or more of the periods of occupation of the Roman fort, and below-ground structures of medieval and post-medieval date.

Summary of results

Ground penetrating radar (GPR) is a geophysical technique that transmits a signal into the ground and senses reflections (like echos in sound) when the transmitted signal hits a change in soil type or buried object. The GPR surveys at Hillside have revealed considerable variation in subsurface reflection patterns, consistent with extensive anthropogenic disturbance and natural variability of the subsurface at the site. Although a number of relatively linear reflective anomalies are noted at the site, perhaps the main finding is the presence of areas of the site that nulls (attenuates or weakens) the GPR signal, perhaps as a result of the presence of subsoil with a very high clay content. The alignment of one such geophysical anomaly appears to follow the orientation of the projected western boundary of the Roman fort and thus may be interpreted as evidence of subsurface structures installed as part of the defensive earthworks.

Method

Georeferencing: All GPR survey grid positioning was carried out using a Trimble R8 GNSS system in RTK survey mode and a Trimble S6 robotic total station. Seven semi-permanent pegs were installed at the site and surveyed to British National Grid usng the Trimble R8. The Trimble S6 was then georeferenced to these pegs, allowing surveying of all geophysical plots and key features at the site.

GPR: MALA ProEx 800MHz, 500MHz & 250MHz antenna. The site was divided into seven rectangular plots (HA, HB, …, HF) in order to accommodate internal boundaries. 3D GPR surveys carried out on all plots using 500MHz antenna. In two plots (HE and HF) 3D GPR surveys carried out with 250MHz antenna and in plot HF, 3D GPR surveys carried out with 800MHz antenna. Additional 800MHz antenna surveys carried out on eight transects in plot HE. All 3D 500MHz surveys (except HF) conducted in orthogonal directions. 3D 250MHz and 800MHz surveys only carried out along longest axis of survey plot. For the 500MHz surveys a total of approximately 3.3km line surveys were carried out. Technical details in Appendix A.

Data Processing

GPR: Radar velocity estimated from hyperbola matching in *ReflexW*. *GPRPy* used for GPR data processing: time-zero correction, survey length correction, dewow, power-law gain. *GPRPy* used to generate 3D model in vts format for viewing in *ParaView*.

Survey conditions
Site cover: Mixed cover at the site: gravel, grass, cobbles. Significant topographic variation at the site (details below). Weather conditions: dry.

1. Site description and context

1.1 The survey was requested by Nigel Neil on behalf of the Lancaster and District Heritage Group (LDHG). The site is adjacent to Scheduled Monument (National Heritage List no. 1020668) '*Part of a Roman fort and its associated vicus and remains of a pre-Conquest monastery and a Benedictine priory on Castle Hill'*. Archaeological excavations had been carried out in two plots at the site (2017 & 2019), revealing possible evidence of historic ditches that could have an alignment with western defences of the Lancaster Roman forts (see Collins, 2020). Wood (2021) outlines current views on the likely north/west extent of the forts. Figure 1 shows the survey area in relation to the Roman fort outlines proposed by Wood (2021).

1.2 The northern part of the site, under the gravel adjacent to the garages (formerly stables), was the original site of what became Lancaster Royal Grammar School. The school there, founded before 1284, and re-built in 1682, was demolished in 1853 (Murray, 1952). Furthermore, there is documented evidence of the use of an area of the site adjacent to the Priory churchyard wall as a unconsecrated malefactors' burial site (see Figure 2). The malefactors' burial ground was established in c. 1700, and was used sporadically until c. 1817. The churchyard was extended down the slope, north of Hillside, in c. 1819 (Nigel Neil, pers. comm., 2023). Nos 4 to 6 Hillside are believed to date from c. 1820, though earlier houses and the school are shown on the site on a map of c. 1685 (the Kuerden or Docton maps; Lancashire Archives DDX 194/16r and 20r). The site has thus experienced significance development and disturbance over extensive periods.

1.3 In 2016 Minerva Heritage Ltd. were commissioned by the owners of No. 4 Hillside to conduct an archaeological evaluation, comprising three small trial trenches in part of the site. The test pits revealed archaeological deposits (some Roman) and potential evidence of human burials. The human remains were noted (left *in situ*) in a location inconsistent with present knowledge of both the churchyard and malefactors' burial ground, though the present churchyard boundary may not be much earlier than the c. 1685 Kuerden map, and a larger medieval churchyard is undoubtedly a possibility. These test pits, along with other archaeological digs at the site contribute to additional disturbance of the site.

1.4 In 2018 RSK carried out a GPR survey in part of the site. Their survey appears to have been focussed on selected 2D transects. The results suggest some localised anomalies (buried linear services or foundations, disturbed ground and in filled ditches) but as 3D surveys were not carried out, no alignment of such anomalies was offered in the RSK report. The exact locations of GPR surveys carried out by RSK is unknown.

1.5 Prior to conducting the geophysical surveys reported here, a topographic survey was carried out to georeference key features (see Figure 3). The area with exposed dressed stone to the southwest of the site (Figure 3) may indicate the extent of the former malefactors' burial area (marked in Figure 2). Figure 3 also shows the position of surface drains and a hydrant. It is not clear how the drains are connected underground (and how they are connected to residences) and the nature/type of any pipework. It is believed that the street drains are either individual soakaways, or linked to a single soakaway, and are not connected to the properties (Nigel Neil, pers. comm., 2023). Note that such services will mask some of the geophysical surveys.

1.6 Figure 4 shows the approximate locations of prior (recent) excavations at the site.

1.7 In total, seven GPR plots were surveyed. These are labelled HA to HF – see Figure 5.

1.8 From numerous spot elevation measurements, a topographic map was produced (see Figure 6). Over 2m elevation change in ground level is evident.

1.9 Figure 7 shows a panoramic photograph of the site; Figure 8 shows a number of photographs taken during GPR surveys.

2. GPR survey results

2.1 Figure 9 shows a horizontal slice of the composite GPR model of the 500MHz data at a depth of 0.3m below ground level. A few features are worthy of note. (1) Stronger reflections are seen in the northeast area of the site (which corresponds to higher elevation of ground level); (2) a linear feature (approx. 10m x 2m) is evident in the northeast area, further north is an almost square shaped anomaly; (3) two patches of strong reflections are seen adjacent to the garages to the northeast of the plot; (4) the reflections are generally weak in plots HD, HE and HF; (5) a near-linear reflection anomaly is seen connecting the two drains in the centre of the site (in plot HE), which appears to marry with the surface gully highlighted in Figure 3.

2.2 Figure 10 shows horizontal slices of the composite model of the 500MHz data at depths of 0.5m, 0.7m, 0.9m, 1.1m, 1.3m and 1.5m below ground level. The main features of note are: (1) the reflection anomaly noted above in the north of the site (plots HB and HC) is evident at 0.5m but at greater depths becomes a weak/null reflection (this is discussed later); (2) on the western edge of plot HC a linear reflector is seen at depths greater than 1m, which may align with the position of the rear wall of the former school building; (3) in plots HE and HF at depths 0.5m and 0.7m a clear linear reflection anomaly runs 2 to 3m away from the Priory churchyard wall in a NNE-SSW alignment - this does not follow exactly the topographic variation (Figure 6) and so is unlikely to be attributed solely to that, it does, however, appear to extend beyond the proposed coverage of the malefactors' burial area but, interestingly, shows an orientation not dissimilar to the expected fortification boundary (Figure 1); (4) at 0.7m depth and deeper, a weak/null reflection is seen in plot HE, again following a NNE-SSW alignment.

2.3 The 250MHz surveys (plots HE and HF), unlike the 500MHz surveys, involved measurements made only in one orientation. This coupled with the fact that antenna footprint is much larger then the 500MHz antenna, the 250MHz data offer little additional information. Figure 11 shows an example depth slice (0.7m) for the 250MHz GPR model.

2.4 The 800MHz survey (plot HF), again, offers little additional information but does show supporting evidence of the NNE-SSW reflection pattern (noted in the 500MHz data) at 0.4m and 0.5m depths (Figure 12).

2.5 Usually, the interpretation of GPR data focusses on the occurrence of reflected signals, however, several areas of the site have revealed patches of weak/null reflection, some of which appear to follow some alignment. And, in fact, close inspection of the processed 2D transects from a number of the plots show interesting behaviour, as illustrated in Figure 13. In this figure, three example transects are shown. Within each transect, the reflection pattern is as expected (e.g. between Y=0 and 9m in the profile for HB at X=0.2m (upper sub-plot in Figure 13). However, for Y>9m in this particular profile, a marked change in reflection pattern occurs – the reflections at depth are noticeably weaker but, perhaps more significantly, an apparent change in frequency of the white-black-white reflections changes (i.e. they appear to get thicker). This is even more evident in the middle sub-plot in Figure 13 (for HB X=2.2m) – between Y=9m and 12m an even greater change in reflection pattern is seen (see also the lower sub-plot for HC X=3.0m between Y=14m and 16m). It appears that in these specific sections of the transect the antenna is coupling differently with the

ground and changing the radar transmission pattern significantly. This can occur when traversing over a region of very high electrical conductivity near the ground surface. Such conditions could be the result of shallow metallic objects (e.g. reinforced concrete (the metal acts as the conductor) or very high clay content in the shallow subsoil).

2.6 The same features noted above are also evident in surveys in plot HE – see examples in Figure 14 (note the striking change in reflection pattern in the lower sub-plot (HE Y=19.8m) between X=4.5m and 6.5m). Figure 15 shows some of the HE plot profiles with topographic correction to further illustrate the lateral contrast in GPR reflections. The reflection patterns on the left of some of the GPR images hint at the possibility of extension of the ditch noted in the smaller LDHG trench (position also marked in Figure 15), but are also aligned with the exposed dressed stone (also marked on Figure 15) and so could be due to burials or demolition of the malefactors' burial boundary wall.

2.7 Given the observations noted above, the composite dataset can be interpreted as consisting of two different types of anomalies: (type 1) zones with strong reflection patterns following some alignment; (type 2) zones with weak/null reflection (and, in some cases significantly altered radiation patterns), that exist in some alignment or in localised patches. The type 2 patterns in plot HE (under the cobbled road) may be interpreted as a result of underground services since there is visible evidence of surface drains. However, these must be metallic for them to cause such behaviour and must extend well beyond (laterally) the alignment of the drains. An alternative, and more likely, interpretation is the presence of extensive zones of clay rich soil. In the lower sub-plots in Figure 10, these form a clear NNE-SSW alignment under the cobbled road of plot HE, whereas at the north of the site, they exist in a region approximately 5m by 5m (plot HB/HC).

2.8 Figure 16 shows a summary of main shallow and intermediate depth features discussed above, along with an approximate orientation of the western boundary of the Roman fort (after Wood, 2021). It should be noted that the three anomalies highlighted in the north and northwest of the site (adjacent to the existing garages) exist in the area of the original grammar school (see Figure 2) and so may be a result of demolishing of said building. The shallow anomalies in the northeast of the site are in the grounds at the front of the former school (e.g. 'playgrounds'). The intermediate depth anomalies (marked in orange in Figure 16) may be consistent with the ditch observed in the small LDHG trench, but could also be a result of demolition of the malefactors' burial boundary wall.

2.9 Given the suggested interpretation of the nulling of the GPR signal under the cobbled road as the result of clay rich subsoil, it is interesting to note that this linear anomaly (rectangle marked in white in Figure 16) is aligned with that of the western fort boundary, leading to speculation that it is a result of remobilised clay presumably installed as part of the western defences (e.g. Jones and Shotter, 1988).

2.10 Figure 17 shows a summary of deeper features. It should be noted that attenuation of GPR signal at shallow depth results in nulling at further depths and thus the 'null anomaly' in Figure 16 at a depth of 1.5m does not necessarily equate to a feature at this depth – it means that a feature at a depth above it results in the attenuation. However, this figure has been included to illustrate the linearity of the contrast between weak and strong GPR signals. Furthermore, observations from the LDHG excavation (approximate position in Figure 16) revealed the presence of a ditch structure (Collins, 2020), adding more support for the interpretation of the presence of former defensive earthworks.

3. Conclusions

3.1 The GPR surveys at Hillside have revealed considerable variation in subsurface reflection patterns. Such heterogeneity is consistent with extensive anthropogenic disturbance and natural variability of

the subsurface at the site. Differentiating specific geophysical features and their cause is challenging because of the progressive disturbance. However, the GPR data show a number of features, perhaps the most intriguing and potentially significant is the apparent presence of shallow high electrical conductivity subsoil that leads to significant nulling of the GPR signal, and in some cases, major transformation of the antenna radiation pattern. Whilst such features could be due to more recently buried (or installed) metallic material, an alternative and more likely interpretation is the presence of soil with a very high clay content. The alignment of one such feature appears to follow the orientation of the projected western boundary of the Roman fort and thus may be interpreted as evidence of subsurface structures installed as part of the defensive earthworks.

3.2 Whilst a great deal of information has been gathered by the geophysical survey, the results presented here and their interpretation should not be relied upon as a sole and complete record of subsurface features present at the site.

Data availability

All the raw GPR data, along with coordinates of surveyed plots (to British National Grid) are available at 10.5281/zenodo.8253179

References

Collins, R., 2020, Roman Britain in 2019: 4. Northern England, *Britannia*, 51, 397-406. DOI: 10.1017/S0068113X20000410

Jones, G.D.B. and D.C.A. Shotter, 1988, Roman Lancaster. Rescue archaeology in an historic city 1970-1975. *Brigantia Monograph* No. 1, University of Manchester, 246 pp.

Murray, A. L., 1952, *The Royal Grammar School, Lancaster: a history*, W Heffer & Sons, Ltd., 369pp.

Plattner, A.M., 2020, GPRPy: Open-source ground-penetrating radar processing and visualization software, *The Leading Edge*, 39 (5), 332-337. DOI: 10.1190/tle39050332.1

Wood, J., 2021, Beyond the Castle: The Archaeology of Lancaster's Castle Hill.

Appendix A. Technical information: Ground Penetrating Radar (GPR).

Instrumentation: MALA ProEx unit with 800, 500 & 250MHz shielded antennae.

The shielded GPR system typically operates in reflection mode: a transmitter antenna provides a pulse of high frequency electromagnetic energy and a receiver antenna records signals travelling directly from the transmitter and from reflections in the subsurface. Surveys are conducted along transects using an odometer to trigger measurements. Seven rectangular survey grids were selected to provide coverage of the site (Figure 5). After laying out a survey grid, survey lines were positioned at equal intervals (0.4m for 250MHz and 500MHz, 0.2m for 800MHz) and transects run in parallel. The process was then repeated in an orthogonal direction for the 500MHz surveys. Sampling along each transect was 2cm. Data were recorded over a suitable time window to capture key reflections (typically 65 to 75ns for 250 and 500MHz, 25ns for 800MHz). The odometer recorded distance for each transect is compared to the known survey length and corrections made, when necessary, to adjust the recorded position, assuming a linear drift. Such errors can occur due to odometer wheel slippage but are typically of the order of a few percent.

Each transect dataset was processed individually in *GPRPy* (Plattner, 2020) using the following steps: (1) odometer correction to known survey length; (2) time-zero correction; (3) dewow (low frequency fiter); (4) time window truncation (to remove later sections of the trace where no reflections are present); (5) application of a gain function (to amplify signals at later times in the trace); (6) translation of time window to an effective depth using an appropriate velocity. In order to obtain a velocity measure, a number of transect datasets with visible hyperbolic reflections were selected for velocity analysis in *ReflexW* (*GPRPy* has this feature too but *ReflexW* has much greater flexibility and user control). The inferred average velocity from such analysis was 0.08 m/ns, although some variation was noted, reflecting the heterogeneity of the subsurface. Most of the observed hyperbolae occur at shallow depth and yet the velocity may vary with depth. Consequently, the computed depths of GPR reflections but be treated with some caution. For example, a two way (i.e. from transmitter to reflector and return to receiver) of 30ns equates to a reflector depth of 1.2m (assuming a velocity of 0.08m/ns). A 10% uncertainty in that velocity equates to a reflector depth range of 1.08 to 1.32m.

Once each transect was processed in *GPRPy*, they were combined (along with orthogonal surveys) to create an interpolated 3D volume of signal strength (higher signals equating to strong reflections). The interpolation was done on a 10cm (horizontal) x 10cm (horizontal) x 3cm (1cm for 800MHz) (depth) grid. The resultant 3D volume was viewed in *ParaView*, allowing horizontal slices to be extracted. As signal weakens with depth a colour scale was uniquely assigned for each depth slice. It is, therefore, important to recognise that a colour for one slice does not necessarily equate to an equivalent signal strength on another slice. Note also that for each depth slice a common colour scale was used. However, it should be noted that ground coupling of the antenna was variable across the site given the different ground cover, which can impact the strength of received signals.

No topographic correction was applied to most of the data reported (but see example with correction in Figure 15). It should be recognised that each GPR depth slice represents a depth from the ground surface and not a true horizontal depth.

Figure 1: Location of survey area. Also shown is the proposed north/west extent of the earlier (1st/2nd century) and later (4th century) Roman fort boundaries (after Wood, 2021).

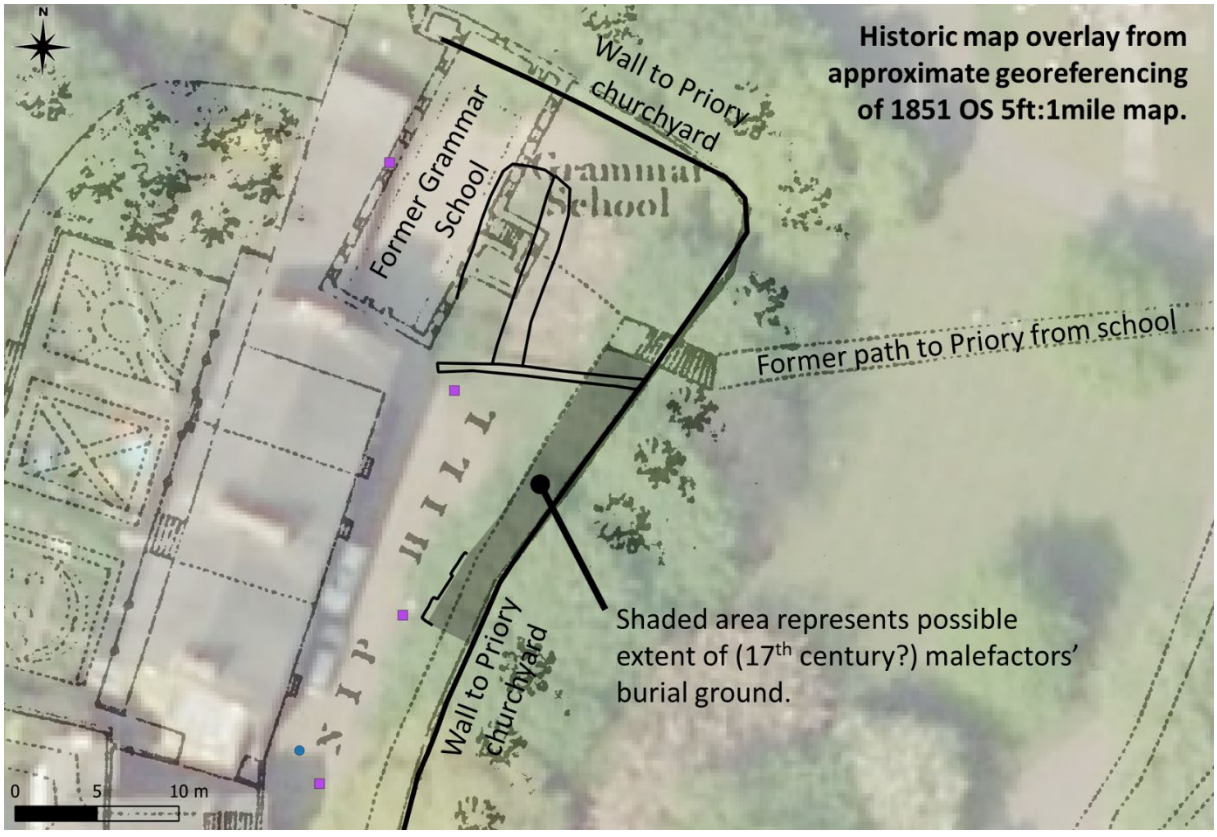

Figure 2: Study site and 1851 OS map overlay showing 18/19th century features at the site.

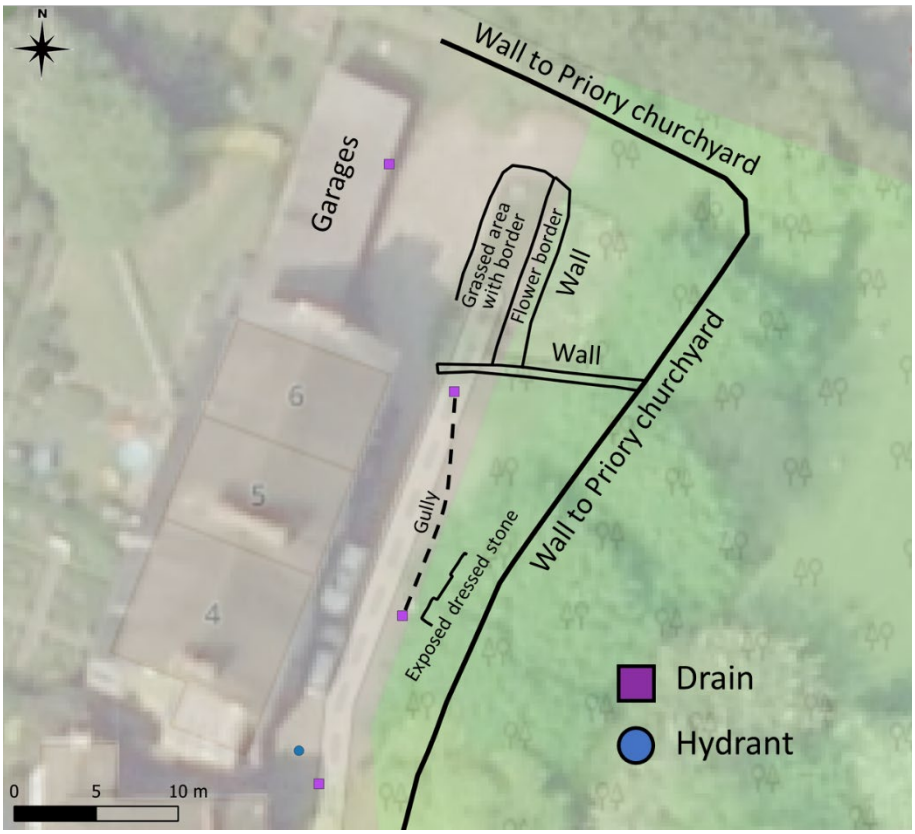

Figure 3: Key features surveyed within the site.

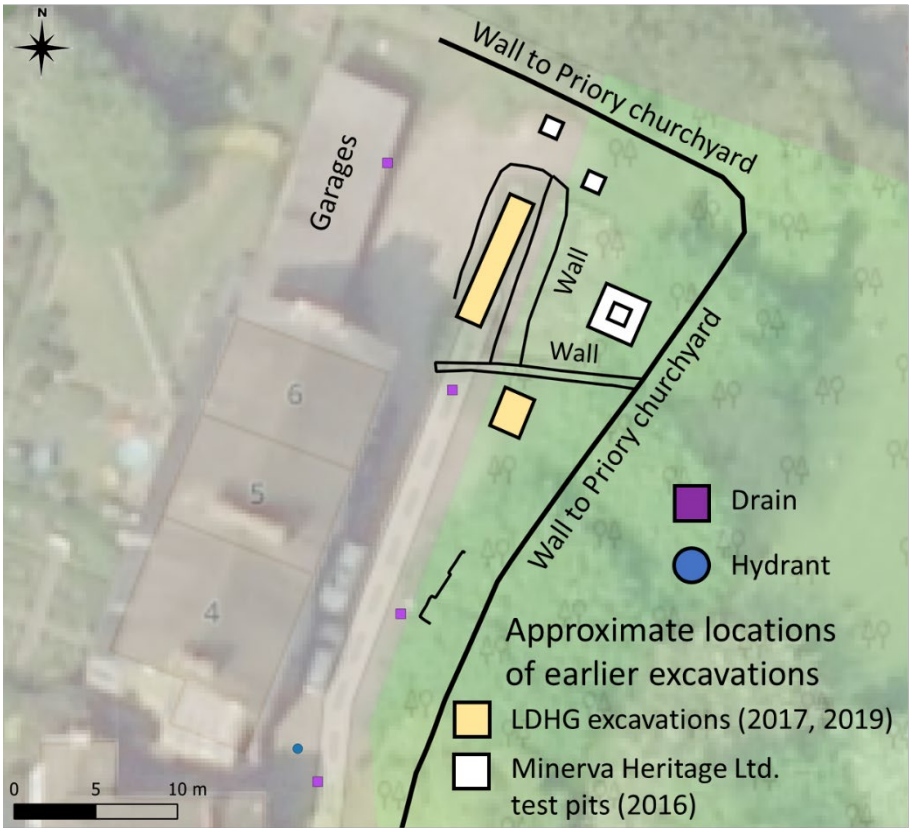

Figure 4: Approximate location of previous (recent) excavations at the site.

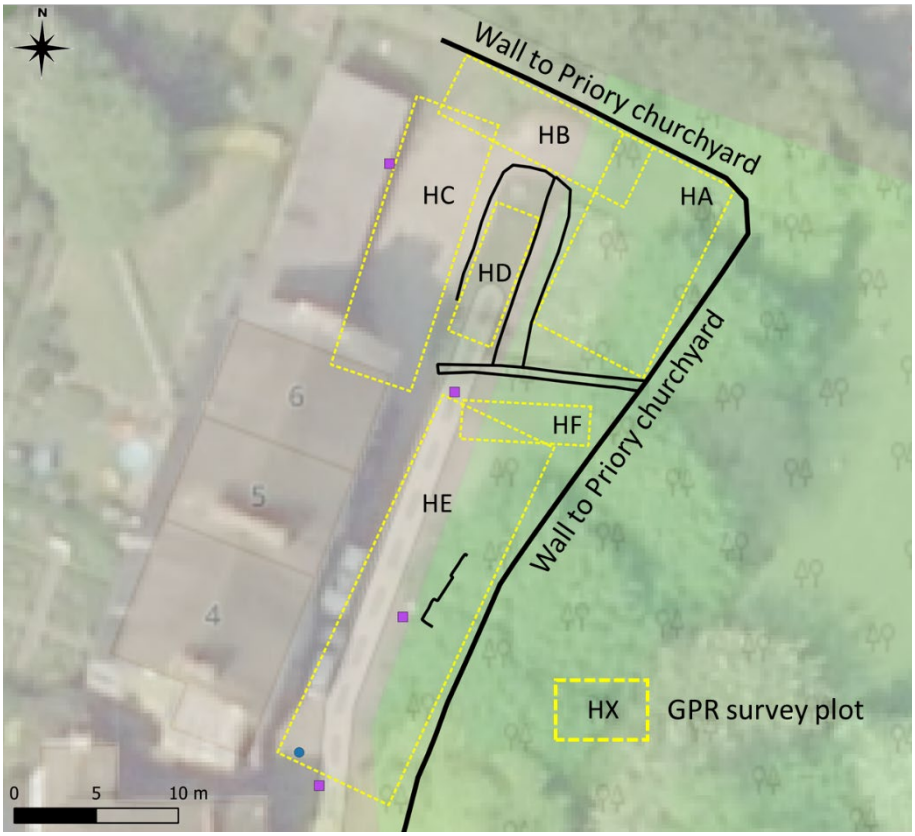

Figure 5: Location of the GPR survey plots.

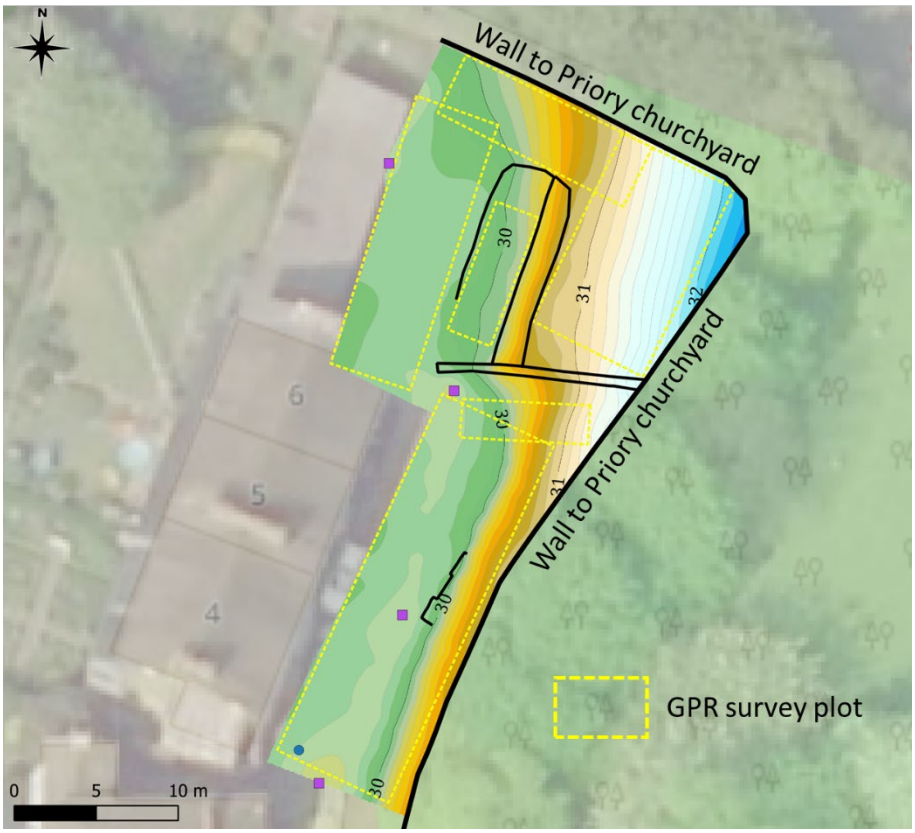

Figure 6: Topographic variation over the site. Contour labels in maOD.

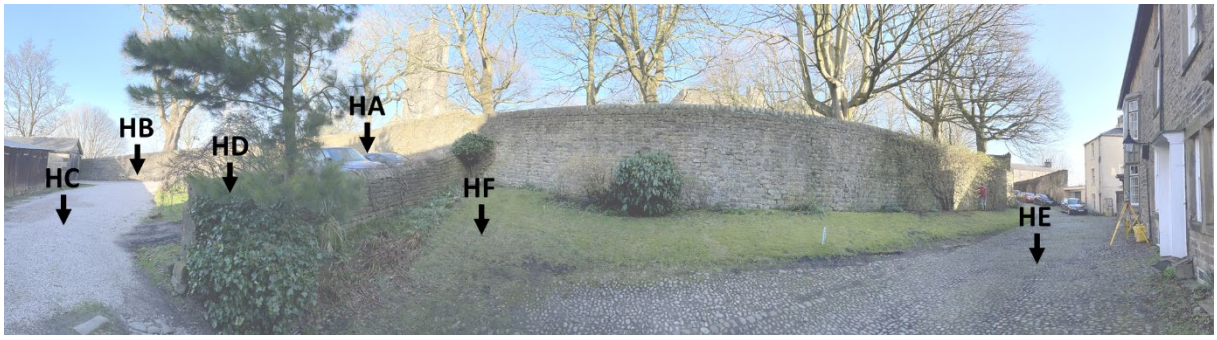

Figure 7: Site photograph showing GPR survey areas.

Figure 8: Site photographs taken during 500MHz GPR surveys.

Figure 9: Horizontal slice of 500MHz GPR model at 0.3m below ground level. Darker colours indicate stronger reflected signals.

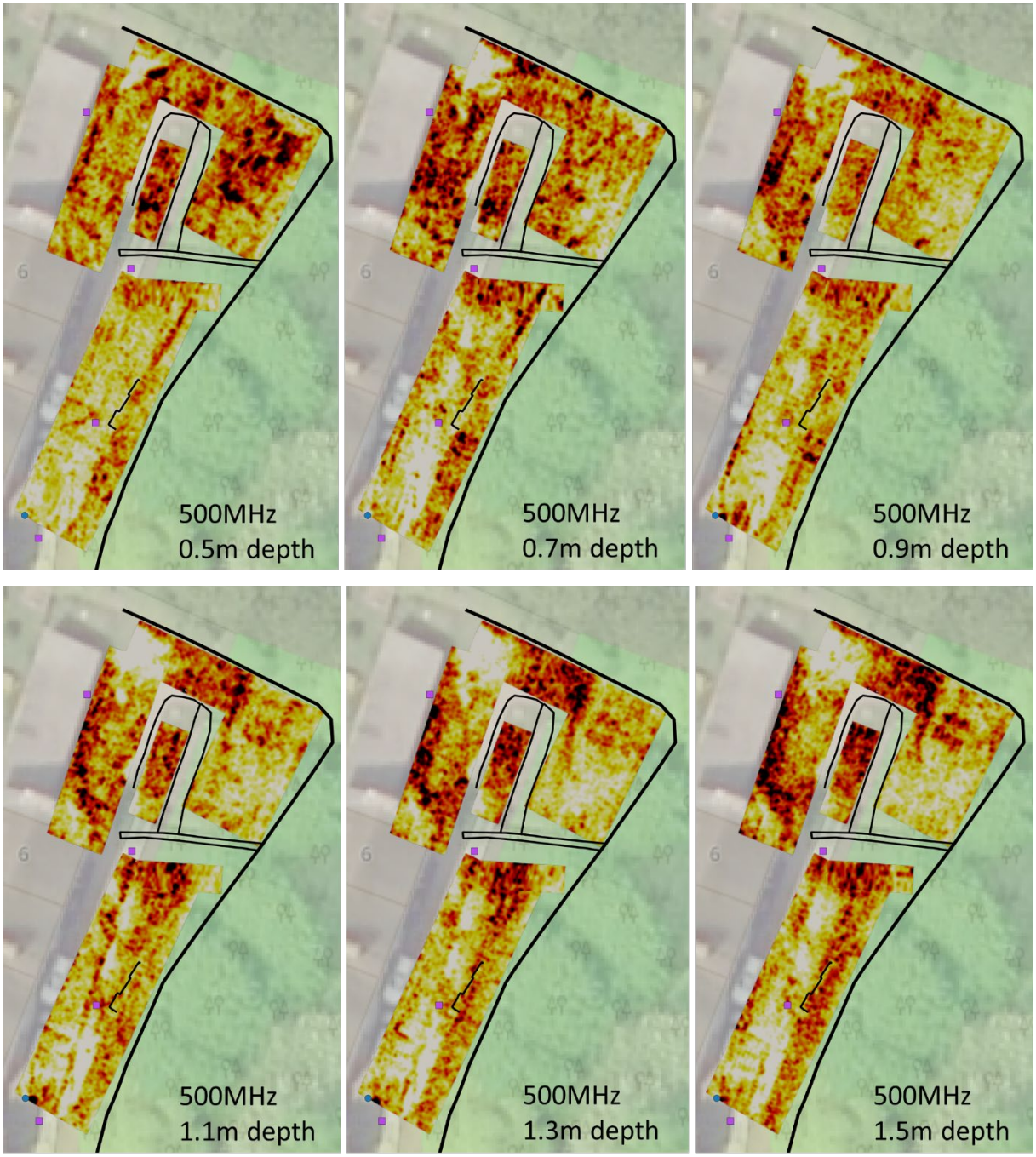

Figure 10: Horizontal slices of 500MHz GPR model at 0.5m, 0.7m, 0.9m, 1.1m, 1.3m and 1.5m below ground level. Darker colours indicate stronger reflected signals.

Figure 11: Horizontal slice of 250MHz GPR model at 0.3m below ground level (GPR plots HE & HF). Darker colours indicate stronger reflected signals.

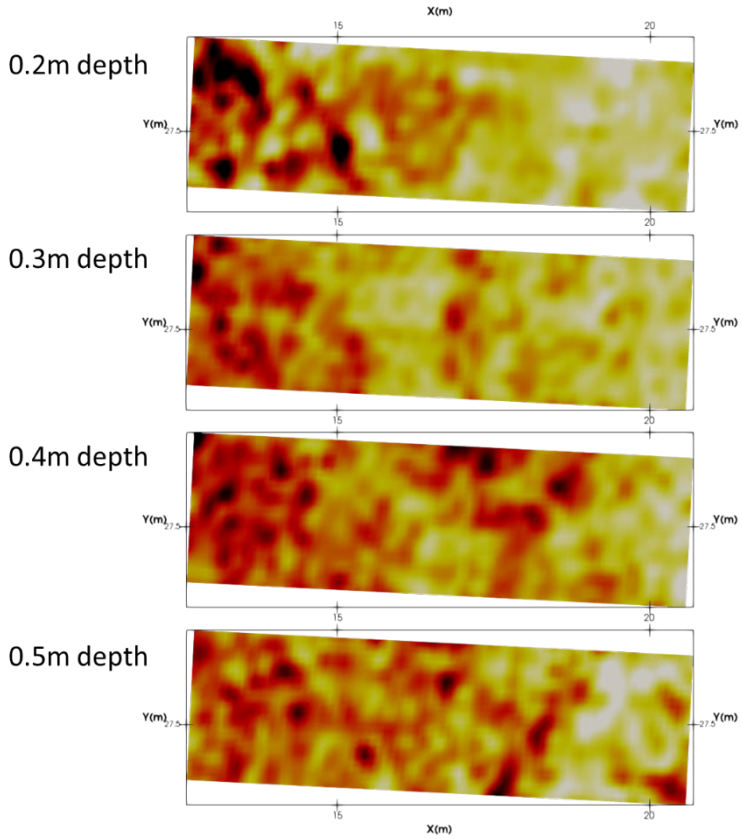

Figure 12: Horizontal slice of 800MHz GPR model (plot HF – see Figure 5) at 0.2m, 0.3m, 0.4m and 0.5m below ground level. X is Easting minus 347260m; Y is Northing minus 461890m. Darker colours indicate stronger reflected signals.

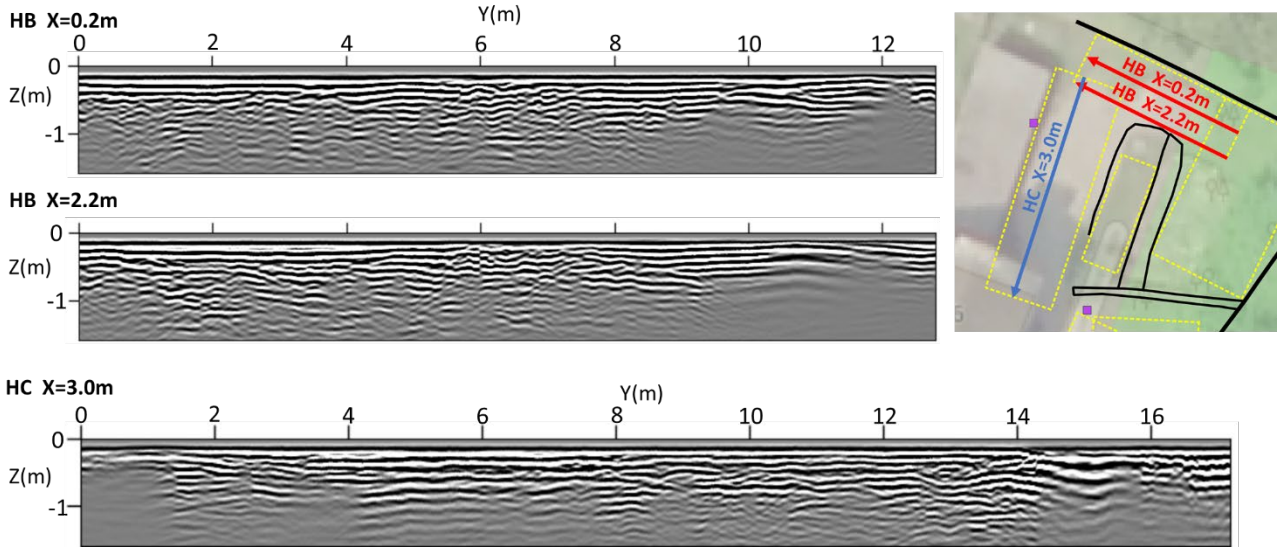

Figure 13: Example 2D vertical slices of 500MHz data in plots HB and HC showing weak/null reflection patterns.

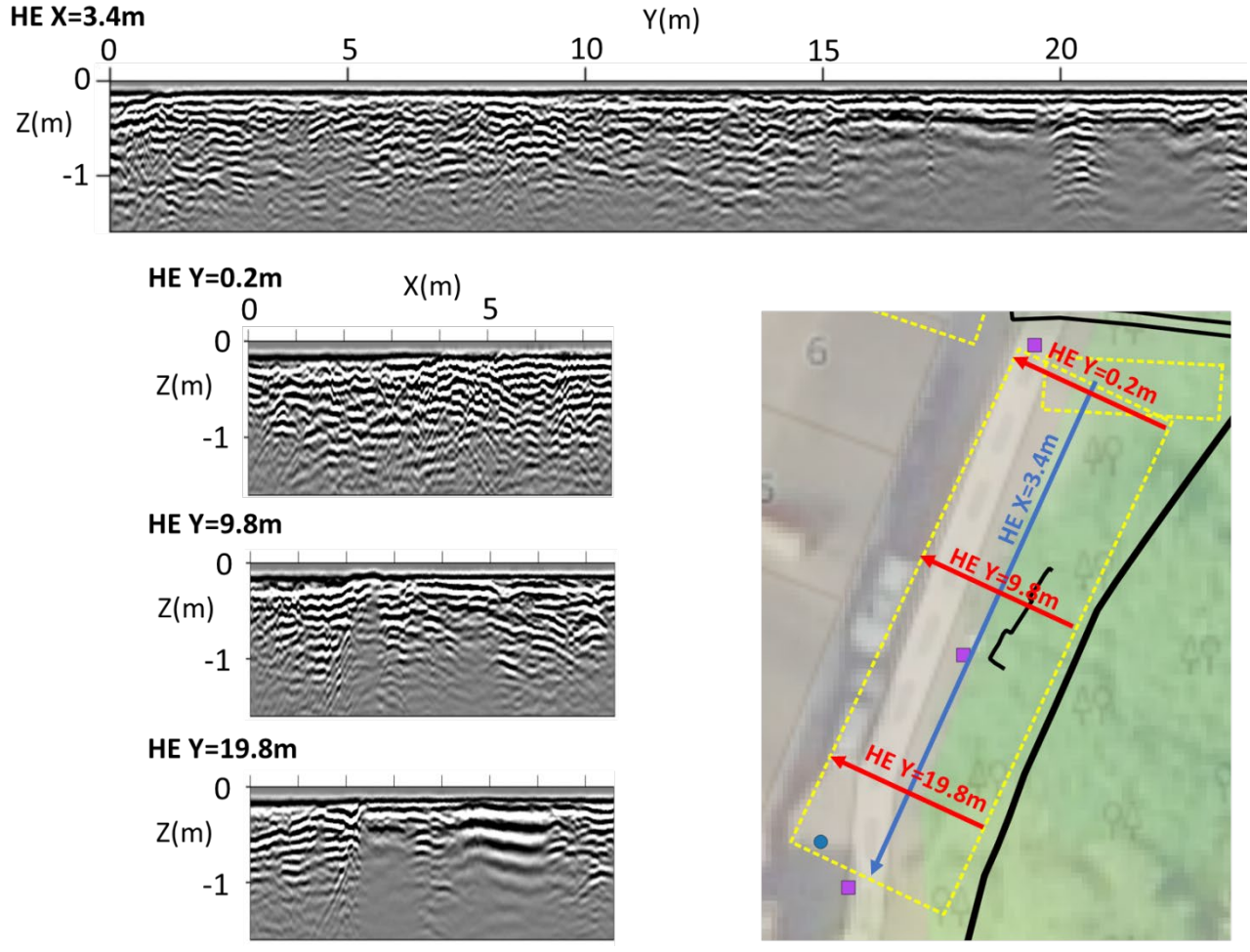

Figure 14: Example 2D vertical slices of 500MHz data in plot HE showing weak/null reflection patterns.

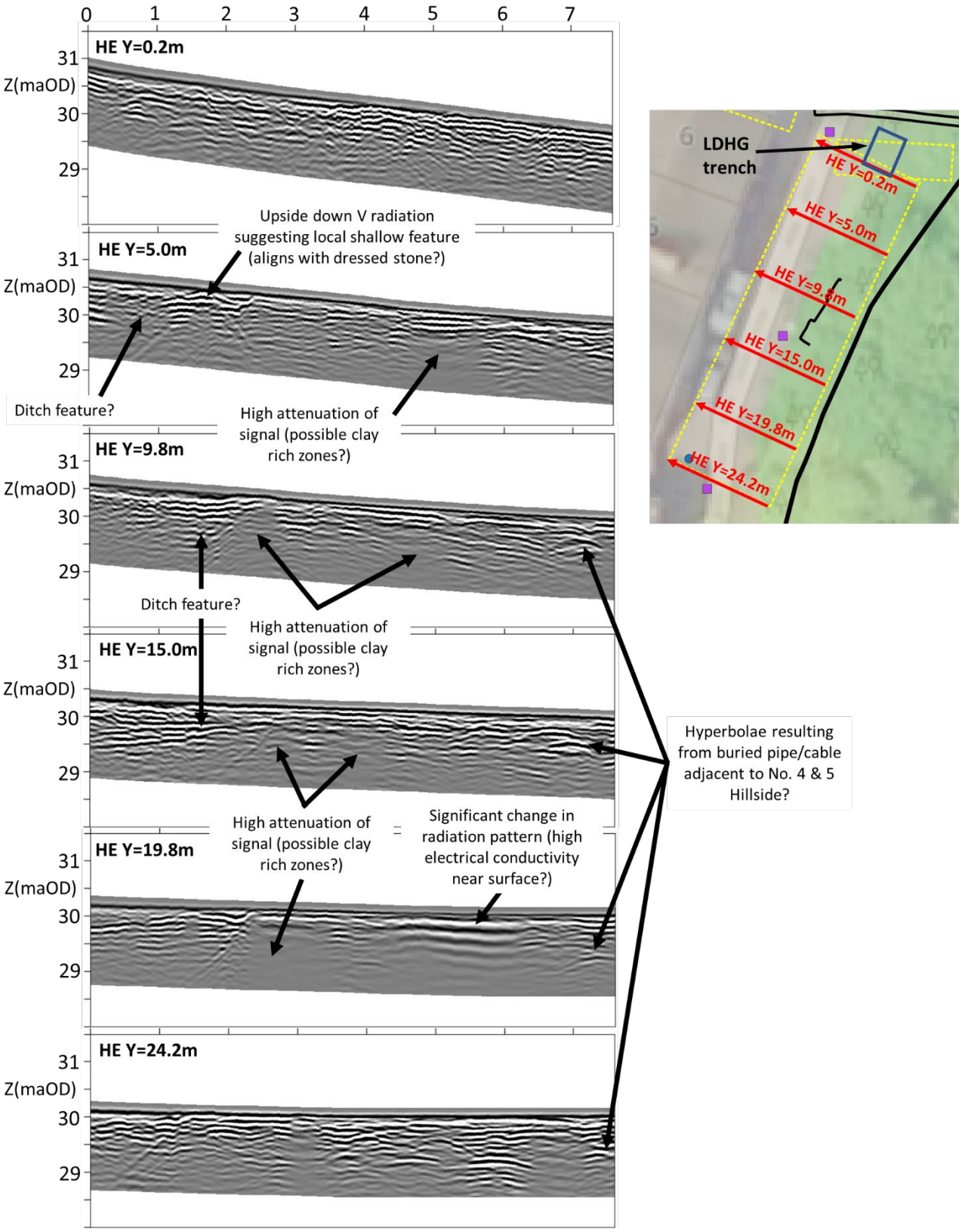

Figure 15: Example topographically corrected 2D vertical slices of 500MHz data in plot HE showing weak/null reflection patterns and other key features.

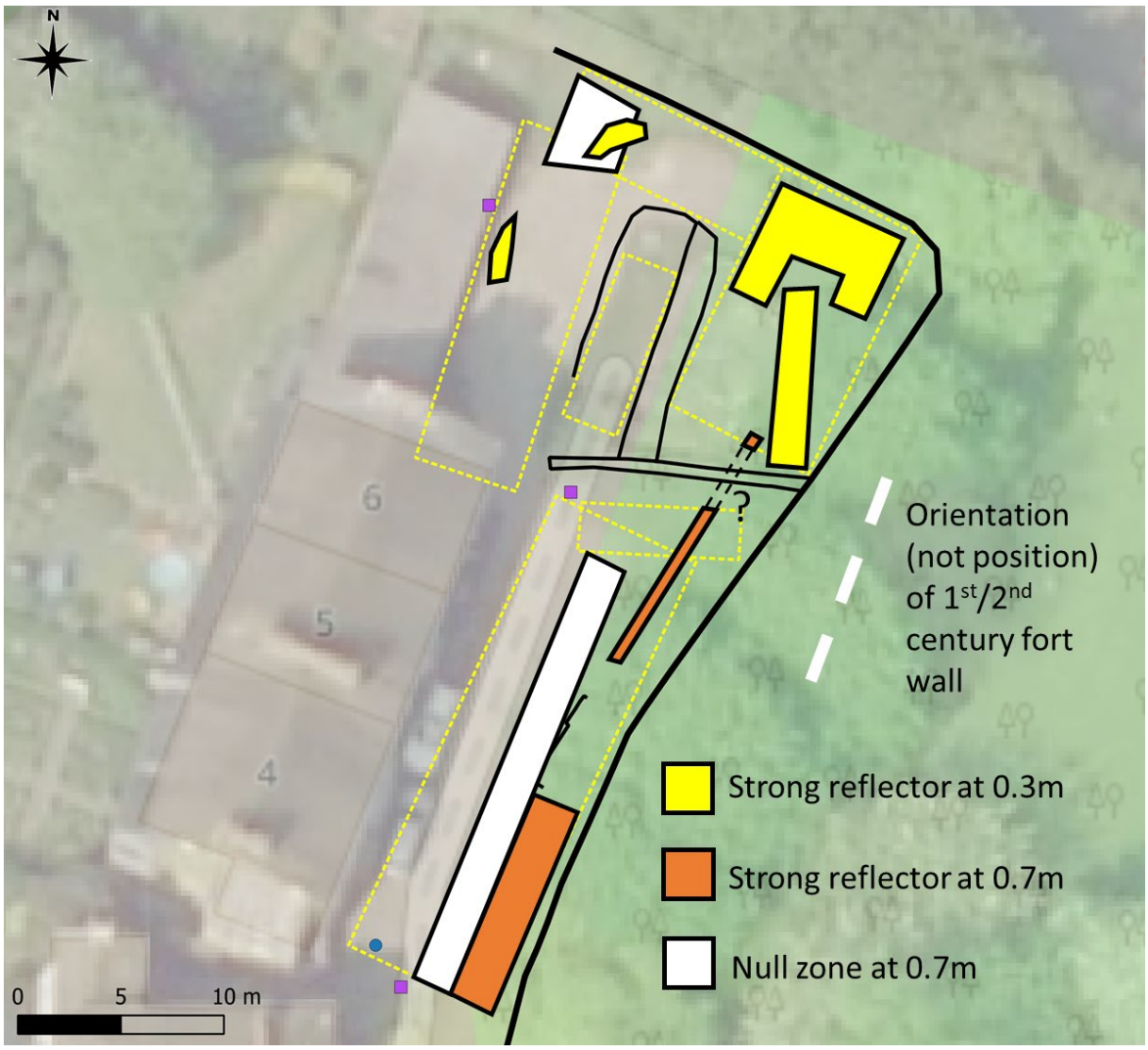

Figure 16: Summary interpretation of main shallow and intermediate depth features. The areas outlined have been highlighted because of their strength or linearity in shape. The approximate orientation of the Roman fort wall (after Wood, 2021) is also shown for reference.

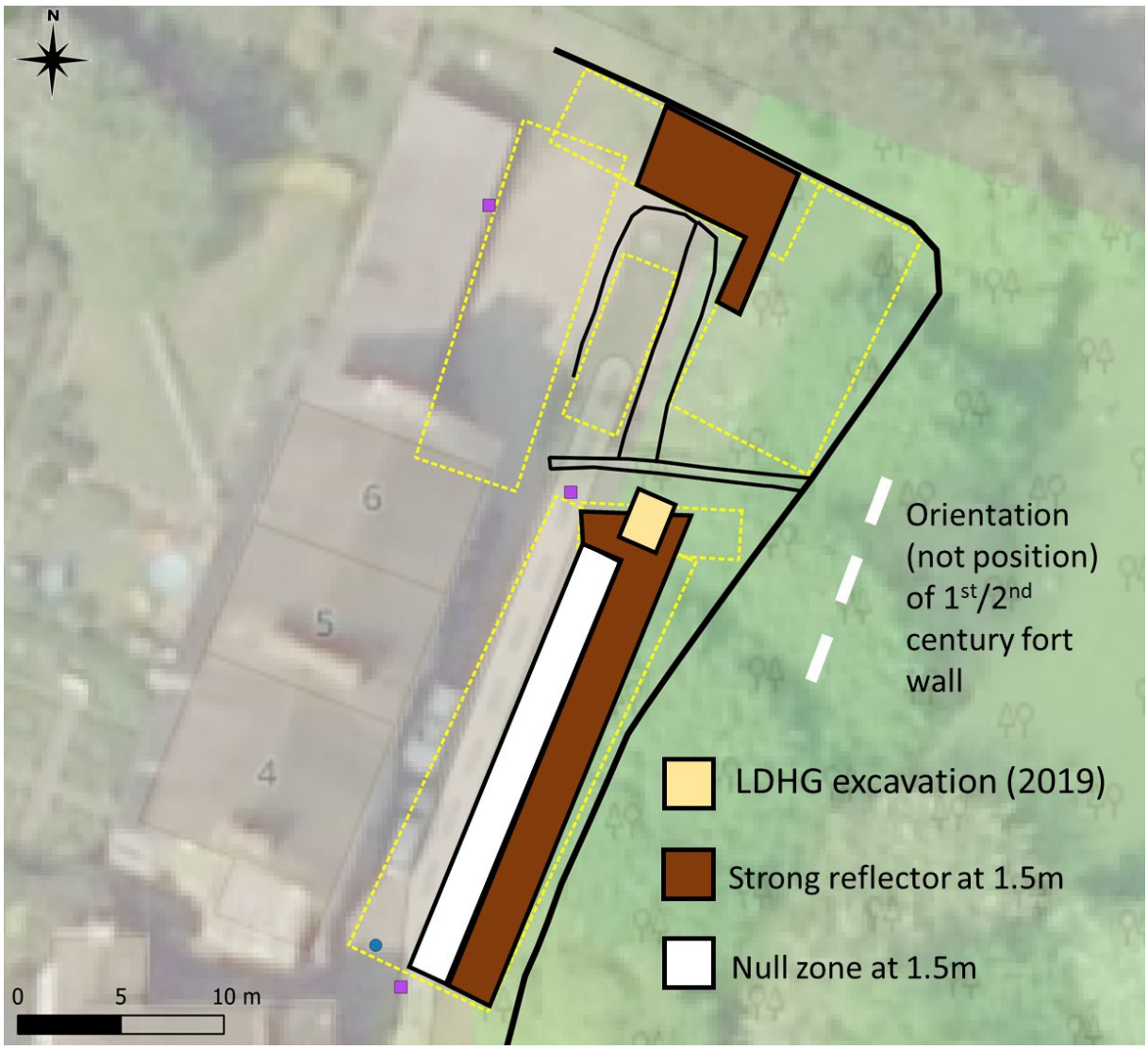

Figure 17: Summary interpretation of deep features. The areas outlined have been highlighted because of their strength or linearity in shape. The approximate orientation of the Roman fort wall (after Wood, 2021) is also shown for reference.